HHS Public Access

Author manuscript

Headache. Author manuscript; available in PMC 2021 October 01.

Published in final edited form as:

Headache. 2020 October ; 60(9): 1961–1981. doi:10.1111/head.13917.

Stimulation of Posterior Thalamic Nuclei Induces Photophobic Behavior in Mice

Levi P Sowers[1,2,3], **Mengya Wang**[4], **Brandon J. Rea**[1,2,3], **Rebecca J. Taugher**[2,5], **Adisa Kuburas**[3], **Youngcho Kim**[6], **John A. Wemmie**[2,3,5,7], **Christopher S. Walker**[8], **Debbie L. Hay**[8,9], **Andrew F. Russo**[1,2,3,6]

[1]Center for the Prevention and Treatment of Visual Loss, Iowa City, IA, USA. [2]Veterans Administration Health Center, Iowa City, IA, USA. [3]Department of Molecular Physiology and Biophysics, University of Iowa, Iowa City, IA, USA. [4]Department of Pharmacology, University of Iowa, Iowa City, IA, USA. [5]Department of Psychiatry, University of Iowa, Iowa City, IA, USA. [6]Department of Neurology, University of Iowa, Iowa City, IA, USA. [7]Department of Neurosurgery, University of Iowa, Iowa City, IA, USA. [8]School of Biological Sciences, University of Auckland, Auckland, New Zealand. [9]Department of Pharmacology and Toxicology, University of Otago, Dunedin, New Zealand.

Structured abstract

Objective: A hallmark of migraine is photophobia. In mice, photophobia-like behavior is induced by calcitonin gene-related peptide (CGRP), a neuropeptide known to be a key player in migraine. In this study we sought to identify sites within the brain from which CGRP could induce photophobia.

Design: We focused on the posterior thalamic region, which contains neurons responsive to both light and dural stimulation and has CGRP binding sites. We probed this area with both optogenetic stimulation and acute CGRP injections in wild-type mice. Since the light aversion assay has historically been used to investigate anxiety-like responses in animals, we measured anxiety in a light-independent open field assay and asked if stimulation of a brain region, the periaqueductal gray, that induces anxiety would yield similar results to posterior thalamic stimulation. The hippocampus was used as an anatomical control to ensure that light-aversive behaviors could not be induced by the stimulation of any brain region.

Results: Optogenetic activation of neuronal cell bodies in the posterior thalamic nuclei elicited light aversion in both bright and dim light without an anxiety-like response in an open field assay. Injection of CGRP into the posterior thalamic region triggered similar light-aversive behavior without anxiety. In contrast to the posterior thalamic nuclei, optogenetic stimulation of dorsal periaqueductal gray cell bodies caused both light aversion and an anxiety-like response, while CGRP injection had no effect. In the dorsal hippocampus, neither optical stimulation nor CGRP injection affected light aversion or open field behaviors.

Conflict of Interest: AFR is a consultant for Lundbeck, Eli Lilly, Amgen, Novartis, Pharmnovo, and Schedule One Therapeutics. DLH is a consultant for Intarcia, Merck Sharp & Dohme and receives research funding from Living Cell Technologies. CSW receives research support from Living Cell Technologies. All other authors have no conflict of interest.

Conclusion: Stimulation of posterior thalamic nuclei is able to initiate light-aversive signals in mice that may be modulated by CGRP to cause photophobia in migraine.

Introduction

Migraine is a complex neurological disorder that is ranked as one of the most disabling diseases worldwide [1, 2]. Many migraine patients have debilitating photophobia that can cause or exacerbate headache [3]. One key player in migraine pathogenesis is the neuropeptide calcitonin gene-related peptide (CGRP) [4–7]. CGRP can induce migraine-like headaches and CGRP levels in the plasma, saliva, and cerebrospinal fluid are elevated during episodic migraine attacks and even between attacks in the case of chronic migraine [8]. Importantly, monoclonal antibodies and small molecules targeting CGRP or a CGRP receptor have proved effective in preventing episodic and chronic migraine for many people [7, 9].

Despite the importance of CGRP in migraine, its sites of action remain elusive. Previous studies have demonstrated that both central and peripheral administration of CGRP can induce light-aversive behavior in mice [10–13]. A key observation was that mice overexpressing a subunit of CGRP receptors in the nervous system (*nestin/hRAMP1*) were light-aversive in very dim light while wild-type mice required very bright light after intracerebroventricular (ICV) injection of CGRP [10, 11, 13]. These data suggest that heightened sensitivity to CGRP in the nervous system increases migraine-associated photophobia.

Within the nervous system, several posterior thalamic nuclei in mice were shown to receive convergent input from nociceptive signals in the dura and light signals originating in intrinsically photosensitive retinal ganglion cells [14]. In humans, corresponding thalamic regions (pulvinar and centromedian nuclei) also receive inputs from non-image forming visual pathways [15]. In addition, neurons in this region were activated in neonatal mice stimulated with bright light [16]. In particular, the ventral posteromedial nucleus (VPM) within this thalamic region is known to contain a CGRP receptor based on immunohistochemical staining and inhibition of neural firing by CGRP receptor antagonists [17]. A role for the thalamus is further supported by imaging studies during migraine [18] and the known role of the thalamus as a relay and integration station in the processing of pain and sensory input [19]. These findings suggest that multiple nuclei within and near the posterior thalamus could contribute to photophobia involving CGRP actions.

One critical aspect of light aversive behavior is that there could be a component of anxiety-like behavior causing a decrease in the time in light. We therefore probed a region of the brain that is involved in aversive and anxiety-like behaviors to better understand if there was a difference between migraine-like light aversion and light aversion that is the result of an anxiety-like response. The periaqueductal gray (PAG) is a key region in pain physiology that is also activated during migraine [20–22]. However, the dorsal region of the PAG (dPAG) plays a critical role in aversive and anxiety-like responses, which include freezing and escape responses in mice [23, 24]. We therefore hypothesized that stimulation of the dPAG could induce both light aversion and an anxiety response.

In this study, the role of posterior thalamic nuclei and dPAG in light-aversive behavior was tested using optical stimulation and stereotaxic injection of CGRP of these regions. While both optical stimulation and CGRP injection into the posterior thalamic region induced migraine-like light-aversive behavior without anxiety-like responses, the same stimulation in the dPAG induced light-aversive behavior accompanied by anxiety-like responses, while CGRP injection had no effect. The same approaches were applied to the dorsal hippocampus, which served as a negative anatomical control because while it expresses CGRP and CGRP receptor components [25, 26], it is not expected to play a direct role in light-aversive behavior and is just superior to the posterior thalamic injection site. The results indicate that the posterior thalamic region is sufficient to induce migraine-like light aversion and may potentially be a site for the actions of CGRP during these migraine-like states.

Materials and methods

Animals

The use of animals is necessary to model migraine-like behavior which is impossible with cell culture or computer models. A total of 270 male and female C57BL/6J mice aged 10–20 weeks were used (Jackson Labs) were used for this study. Male mice had an average weight of 20–25g and females were 18–22g. However, no behavior differences were found between the sexes and therefore were analyzed together (data not shown). Mice were housed in groups of 3–5 per cage except when fitted with a cannula, in which case they were housed individually with standard University of Iowa rodent bedding for all mice. *Calca-cre* mice have *cre* inserted into exon 2 of the *Calca* gene and were kindly provided by R. Palmiter [27]. All behavior experiments were performed between 8:00 am and 5:30 pm. For all experiments, mice from the same cage were randomly assigned to either control or experimental groups and investigators were blinded to genotype and treatment. Animal procedures followed the ARRIVE guidelines and were approved by the appropriate animal care and use committees and performed in accordance with the standards set by the National Institutes of Health.

Stereotactic injection of CGRP, Evans blue dye, and red beads

Rat α-CGRP (Sigma Catalog number: 96827–03-1) (5 μg/μl, 2.5 μg/μl, or 0.5 μg/μl mixed in 1X phosphate buffered saline (PBS)) or 1X PBS (vehicle) was unilaterally injected through a small burr hole, into either the posterior thalamic region, dorsal hippocampus, or dPAG. Injection was at 200 nl/min for 1 min (Micro4, Model UMC4 pump), using a 10 μl gas tight Hamilton syringe with a 30-gauge needle. The site of CGRP injection was identified by injection of Evans blue dye (1% dye, diluted in 1X PBS) using the same volume (200 nl) and rate as CGRP injections, into the appropriate brain area of C57BL/6J mice. For all acute CGRP injections, mice were monitored continuously after coming out of anesthesia until behavioral assays were performed. No analgesia was given to the mice as the goal was to assess light-aversive phenotypes and it is possible that analgesics could interfere with the primary outcome. All mice were awake and behaving normally (including eating and drinking) by 30 min post injection.

Bilateral Evans blue dye injections were done in 15 mice separate from those tested for behavior. Mice were anesthetized with 5% isoflurane in an induction chamber; 1.5–2% isoflurane was then applied via a stereotaxic nose cone to maintain anesthesia during injection. Coordinates for the posterior thalamic injections were: anterior/posterior (AP), −0.18 cm posterior to bregma; medial/lateral (ML), −0.11 cm lateral to the midline; and dorsal/ventral (DV), −0.32 cm from pial surface. Coordinates for the dorsal hippocampus were: AP, −0.15 cm posterior to bregma, ML, −0.10 cm lateral to the midline, DV, −0.12 cm from the pial surface. Coordinates for the dPAG were AP, −0.38 cm posterior to bregma, ML, −0.06 cm lateral to the midline, DV, −0.17 cm from the pial surface. The needle was left in place for an additional 5 min after injection before removal. 1 h post injection, mice were subjected to behavioral experiments and then immediately euthanized via CO_2. For the targeting injections of Evans blue, mice were given a 1 h recovery period before being transcardially perfused. For the dPAG, injection sites were also confirmed with red beads (Red Retrobeads™, LumaFluor, Inc.) injected at the coordinates listed above. Following red bead injection, with or without CGRP, and behavioral analysis, mice were perfused and analyzed for the injection site. Mice were perfused with 4% paraformaldehyde in 1X PBS using standard procedures. The brains were cut into 100 μm coronal slices and mounted onto Superfrost Plus slides (Fisher Scientific). Images were acquired using a light microscope (Olympus, CKX41) equipped with an Infinity 1 camera and processed using the INFINITY ANALYZE software (Lumenera Corporation).

To determine the spread of injected CGRP and confirm the presence of CGRP binding sites within the posterior thalamic region, five mice were injected unilaterally with 1 μg (200 nl mixed in 1X PBS) of fluorescein-15-CGRP, as previously described [29]. The same parameters were used as for CGRP injections described above. At 1 h post injection, mice were perfused as described above. Brains were then extracted and processed for immunohistochemistry, as described below. Slices were counter stained with DAPI and imaged on a Zeiss 880 confocal microscope (Zeiss Corporation).

Optogenetic stimulation of specific brain regions

Channelrhodopsin-2 (ChR2) was expressed by unilateral injection of adeno-associated virus (AAV) containing a fusion between ChR2 (E123A) and an eYFP reporter, with expression driven by the calmodulin kinase II (CaMKIIa) promoter (AAV2-CaMKIIa-hChR2(E123A)-eYFP), or the vector control (AAV2-CaMKIIa-eYFP), both from University of North Carolina Vector Core, in the posterior thalamic nuclei and the dorsal hippocampus. A similar expression vector with the pan-neuronal synapsin promoter (AAV2-hSyn-hChR2(E123A)-eYFP), or vector control (AAV2-hSyn-eYFP), also from University of North Carolina Vector Core, was used in the dPAG. Injection volume was 0.4 μl, and the posterior thalamic nuclei, dPAG, and dorsal hippocampus were targeted using the coordinates listed above. Following virus injection, an optical fiber (4.5 mm length for posterior thalamus, 2 mm for dPAG and dorsal hippocampus, 200 μm core diameter, numerical aperture of 0.22, Doric Lenses) was implanted 0.04 cm dorsal to the injection coordinates for the relevant brain region and affixed with dental cement and super glue. Behavioral experiments were performed 3 weeks following surgery to allow for adequate viral transduction. For optical stimulation, mice were connected to a diode-pumped, solid-state laser (473 nm, 300 mW, OptoEngine LLC)

and stimulated at 20 Hz, 5 ms pulse width during fifteen 1 min epochs, each preceded by 1 min without stimulation. Following all behavioral testing, animals were sacrificed, and the accuracy of virus targeting and fiber optic probe tip placement were assessed histologically. For the dPAG, 10/10 probes were immediately dorsal to the PAG or in the PAG. For the dorsal hippocampus, 11/11 fiber optic probe tips were either in the dorsal hippocampus or in the dorsal border of the hippocampus, which was considered a 100% success rate as light shines down into the hippocampus from this location.

Immunohistochemistry

C57BL/6J mice were deeply anesthetized with ketamine/xylazine (87.5 mg/kg/12.5 mg/kg, IP) and perfused transcardially with 1X PBS and 4% paraformaldehyde. The brain was dissected and post-fixed in 4% paraformaldehyde for 24 h at 4°C, followed by sequential equilibration in 10%, 20%, 30% sucrose (at 4°C and 24 h per concentration). Brains were embedded in tissue-freezing medium (General Data Company), stored at −80°C until use, then coronally sectioned at 30 μm. For staining, free-floating sections were rinsed in 0.1 M phosphate buffer (PB) (0.08 M Na_2HPO_4, 0.02 M NaH_2PO_4, pH 7.4), three rinses at 5 min per rinse, and then blocked in 0.1 M PB with 10% goat serum (Sigma, G9023) and 0.3% Triton-X-100 for 1 h at 4°C. Sections were incubated with rabbit anti-CGRP antibody (Sigma, C8198) at 1:2000 dilution at 4°C overnight. After 3 washes in 0.1 M PB with 10% goat serum and 0.3% Triton-X-100 for 5 min each, sections were incubated with goat anti-rabbit Alexa 488 (Thermo Scientific, A11070) at 1:1000 dilution for 1 h at 4°C in the dark. Following staining, sections were rinsed in 0.1 M PB with 10% goat serum and 0.3% Triton-X-100, 2 rinses at 5 min per rinse, then 0.05 M PB, 2 rinses at 5 min per rinse, before being mounted with Vectashield containing DAPI (Vector Laboratories). Images of tissue sections were captured using a Leica Y15P confocal microscope.

Light/dark and motility assays

The testing chambers were a Plexiglas open field (27 cm wide, 27 cm deep, 20.3 cm high) containing three sets of 16 beam infrared arrays (two sets of perpendicular beams cross at a height of 1.0 cm to detect mouse location and locomotion, and the third beam crosses the width of the chamber at a height of 7.3 cm to detect vertical activity) (Med Associates). The field was divided in two equal-size zones by a dark insert (Med Associates), which is a five-sided, black-colored Plexiglas box with a top, but no floor. The use of infrared light beams allowed tracking in both zones. An opening (5.2 cm, 6.8 cm) in the dark insert allowed free movement between zones. A computer using Activity Monitor v6.02 (Med Associates) was used for recording data from the six chambers. The assay using optogenetics was changed as follows. Wild type mice were tested at 2.7×10^4 lux and 55 lux for the posterior thalamic studies and at 2.7×10^4 lux only for the dPAG and hippocampus. Mice (at either light intensity) were tested without pre-exposure to the chamber. The chamber was modified with a small porch and an embedded optical commutator (Doric Lenses) so that mice fitted with an optical fiber could move freely between the light and dark sides of the chamber. The modified dark chamber dimensions were as follows: the opening was 5.08 cm wide x 5.08 cm tall with a small slit running from the top of the opening to the top of the insert, which was 10.16 cm high and 0.95 cm wide. A porch was built from the front of the insert, extending 6.5 cm over the light area. The optical commutator scaffold had an inner diameter

of 1.70 cm. The slit caused only a small change in the light allowed into the dark chamber. In the unaltered dark chamber, the back-right corner received 14 lux, whereas the corner in the chamber altered for optogenetics received 17 lux in the 2.7 X 10^4 lux condition. Data were collected for 30 min and analyzed in sequential 5 min intervals; time spent on each side of the chamber per 5 min interval was averaged. Resting time was measured and normalized to total time spent in either the dark or light zones. Resting time is defined as the time the mouse spent not moving over the time spent in either the light or dark zone. It is a measurement of movement during the light dark assay.

Open field assay

This assay was performed to assess the contribution of anxiety-like behavior in a light-independent assay. For optogenetic experiments, the mice were tested in same boxes used for the light dark assay, but in the open with room lighting (~1000 lux) to avoid having the fiber optic cable restrict their movement (the commutator used to avoid this problem in the light dark assay could not be used since it is part of the dark insert). For acute CGRP injections, mice were run at 55 lux in the boxes. For both conditions, mice were placed in the center of the chamber but without a dark insert. Mice were tested for time spent in the center vs periphery of the chamber over a 30 min period. The periphery was defined as 4.22 cm from the border; the remaining 18.56 × 18.56 cm area was defined as the center. One hippocampal optogenetic experiment was performed using a chamber for which the periphery was defined as 3.97 cm from the margin and the center as 19.05 × 19.05 cm. Data from the experiment with a larger and smaller center were not statistically different (data not shown) and thus were combined.

Experimental design and statistics

All experiments were preformed between 8 am and 4 pm. For all behavioral assays, mice were brought to the room 1 h before experimentation to habituate. For optogenetic studies, mice were allowed 3 weeks to recover from surgery and fully express the viral construct. During that three-week period, mice implanted with the optical fiber probe were singly housed to avoid damage to the optical fiber probe and injury to the mouse. On the behavioral day, animals were split into equal groups of control and experimental viral constructs and the experimenter was blinded. For optogenetic mice, light/dark assay was run first, followed two days later by the open field assay. For acute injection of CGRP, all animals were randomized in cages and a blinded experimenter injected either CGRP or PBS. Cages were split evenly. Mice were used for a single assay and then euthanized.

Power analyses were calculated based on previous studies from the lab and used ClinCalc.com. Effect size for this study was estimated to be 33% for light aversion. An alpha of 0.05 was used and a power of 0.80. These parameters suggested a sample size of around 10 animals in each group. All statistical analyses were performed with GraphPad Prism 8.01 and are presented in Table 1. Error bars represent ± SEM. A total of 12 mice over all experiments were excluded due to tangling of optical fiber or the loss of the fiber optic probe during the assay. This resulted in 6 eyfp and 3ChR2 mice being removed in the optogenetic bright light condition and 2 eYFP mice in the optogenetic low light condition.

All statistical analyses were two-tailed unless stated otherwise. All experiments were repeated at least 2 independent times with different cohorts.

Results

Direct optical stimulation of posterior thalamic nuclei induces light aversion

There are multiple nuclei throughout the posterior thalamic region that contain light and/or dural sensitive neurons, such as the posterior complex of thalamus (PO), VPM, lateral posterior nucleus of the thalamus (LP), lateral dorsal nucleus of the thalamus (LD), and central lateral nucleus of the thalamus (CL). In addition, the VPM and ventral posterolateral nucleus of the thalamus (VPL) contain neurons that are sensitive to sagittal sinus stimulation [14, 16, 17]. These data suggest that the posterior thalamic region is an integration center for light and pain. We therefore asked if optical stimulation of posterior thalamic nuclei centered on the PO could induce migraine-like phenotypes in wild-type mice.

The posterior thalamic nuclei were injected with a ChR2 vector (AAV2-CaMKIIa-hChR2(E123A)-eYFP) that contains a ChR2-eYFP expression cassette driven by the CaMKIIa promoter or a control vector (AAV2-CaMKIIa-eYFP) that only expresses the eYFP reporter. CaMKIIa is well characterized in glutamatergic neurons of the thalamus and we therefore chose the CaMKIIa promoter to increase the likelihood of targeting glutamatergic neurons of the posterior thalamic nuclei [30] although we acknowledge that other neuronal types could be targeted as well. In all assays, separate analyses of male and female mice did not reveal any significant sex differences.

Mice were optically stimulated at 20 Hz for alternating 1 min on/off epochs during the 30 min testing period using 10mW power at the optical probe tip. The mice injected with the ChR2 vector spent more time in the dark relative to eYFP vector controls (Fig. 1). The magnitude of this effect was similar in dim (55 lux) and bright (2.7×10^4 lux) light (Fig. 1A, B) (three-way ANOVA $p>0.05$). The intensity of the dim light is comparable to dark overcast day and the bright light is comparable to a bright sunny day in the shade [31].

There was no change in resting in the light zone regardless of light intensity (Fig. 1C). In contrast, optical stimulation of the posterior thalamic nuclei increased resting in the dark at both light intensities (Fig. 1D), mimicking the effect of CGRP following ICV and IP injections [10–13]. This increased resting in dark relative to light may be analogous to the increased resting by humans with migraine who go into dark rooms and rest to relieve headache pain. Importantly, center time in the open field test was not affected, suggesting that the decrease in time in light was not due solely to anxiety-like behavior (Fig. 1E). The accuracy of posterior thalamic nuclei targeting was confirmed by expression of the eYFP reporter (Fig. 1F, left panel). Optical fiber tips for all ChR2 mice were histologically localized. All 29 mice had viral expression and optical fiber probe tip in the posterior thalamic nuclei, with the fiber optic probe tip specifically in the PO in 15/29 (51%), in the LP in 11/29 (38%), and in the CL in 3/29 (10%). Comparison of the individual mice with placements in the PO, LP, or CL did not reveal any significant behavioral differences (data not shown). The locations are marked with black (2.7×10^4 lux mice) and yellow (55 lux mice) in the Allen Mouse Brain Reference Atlas section most closely matching the targeted

location (Fig. 1F, middle panel). Consistent with a previous report [14], eYFP-positive projections from the posterior thalamic nuclei were observed in the somatosensory cortex (Fig. 1F, right panel). Taken together, these data demonstrate that optical stimulation of posterior thalamic nuclei is sufficient to induce light-aversive behavior in both low and bright light settings.

CGRP-positive fibers are widely dispersed in the posterior thalamic nuclei

We next sought to understand if CGRP in the posterior thalamic region might be involved in these light-aversive responses. To determine which nuclei in the posterior thalamic region are the most likely targets of CGRP, the sites of endogenous CGRP expression in this region were determined. Previous studies had reported CGRP staining in fibers of the VPM [32] and cells of the nearby subparafasicular nucleus [33, 34]. However, it was also reported that CGRP was not detectable near neurons in the posterior thalamic nuclei that are sensitive to both light and dural signals [32]. Therefore, it was important to resolve the distribution of CGRP-containing cells and fibers at the posterior thalamic region coordinates used in this study. Clear CGRP immunoreactive staining was identified within the posterior thalamic region (Fig. 2), although the signals were considerably weaker than in other brain regions, such as the nearby central nucleus of the amygdala (Fig. 2A inset, white arrowhead). CGRP-positive fibers, but not cells, were present in all posterior thalamic nuclei (Fig. 2B). As a control, CGRP antibody staining was validated using homozygous *Calca-cre* (*Calca*$^{cre/cre}$) mice, which do not express α-CGRP [27]. CGRP staining of the posterior thalamic region was not detectable in the *Calca*$^{cre/cre}$ tissue (Fig. 2D) but was in wild-type mice (Fig. 2C). In addition, pre-incubation of the antibody with excess CGRP (10 times the concentration of antibody) blocked staining of the posterior thalamic region (Fig. 2E). These data clearly demonstrate that CGRP-containing fibers are widespread throughout the posterior thalamic region, albeit at relatively low levels.

CGRP injection into the posterior thalamic region induces light-aversive behavior without causing an anxiety-like phenotype

To test the hypothesis that CGRP could be acting in the posterior thalamic region to induce light aversion, CGRP was unilaterally injected into male and female wild-type C57BL/6J mice. Mice were tested 1h post injection. A dose response analysis across a range of 0.1–1.0 μg CGRP showed that light-aversive behavior was induced at all concentrations (Fig. 3A, B). Interestingly, the mice were light-aversive in dim light (55 lux), while after ICV CGRP injection, bright light (2.7×10^4 lux) was required [10]. As also seen with ICV CGRP, the mice rested more, but only in the dark, not the light (Fig. 3C, D). In the light, resting actually decreased, but this was significant at only an intermediate dose (Fig. 3C). Importantly, there was not any difference upon CGRP treatment in center avoidance in the open field assay, suggesting that the injection of CGRP into the posterior thalamic region does not induce anxiety-like behavior (Fig. 3E). As with optogenetic stimulation, there were no significant differences between male and female mice in the behavioral assays. Injection of Evans blue dye in a separate cohort of mice was done to confirm targeting accuracy in the posterior thalamic region, with a representative image shown in Fig. 3F. Of those injections, 23 out of 30 bilateral injections were centered in the PO, and all were within the posterior thalamic nuclei. Thus, injection of CGRP into the posterior thalamus induced light-aversive behavior

at low light intensity and led to a greater propensity to rest in the dark, but not the light, without leading to an increased anxiety-like phenotype.

Identification of CGRP binding sites and peptide spread in the posterior thalamic region

Neuropeptides are known to travel long distances after release while neurotransmitters are rapidly broken down at the synapse [35]. To determine how far the largest amount of injected CGRP (1 μg in 200 nl) could spread in the posterior thalamic region, the same amount and volume of a fluorescent CGRP derivative was used (Fig. 4). Fluoroscein-15-CGRP (fluoro-15-CGRP) has recently been shown to be a full agonist, although with reduced potency at the CGRP receptor when measured by cAMP production in a HEK293 expression system [29]. Using this ligand gave the added benefit of confirming the presence of CGRP binding sites within the posterior thalamic region, although with the reduced affinity it is likely that not all sites will be detected. The caudal and rostral borders of fluoro-15-CGRP spread is represented in Fig. 4A and 4C, respectively, where very dim fluorescence can be observed (white arrowheads). There was some variability in the spread of fluoro-15-CGRP, with the largest spread covering the entire posterior thalamic region, including additional nuclei beyond the posterior thalamus. (Fig. 4B right panel, blue shading) and the smallest spread covering about 1/3 of the total posterior thalamic region (Fig. 4B right panel, purple shading). The image in Fig. 4B represents the largest spread we observed with the injections. Interestingly, clusters of fluorescent binding on cell bodies can be observed in several posterior thalamic nuclei, especially within the PO (Fig. 4B insets 1 and 2), suggesting that fluoro-15-CGRP is binding to receptors on these cells.

Optical stimulation of the dPAG induces significant light-aversive behavior with anxiety while CGRP injection induces no change in light-aversive behavior

Thus far, the data implicate CGRP-sensitive neurons in the posterior thalamus in light-aversive behavior consistent with their previously reported sensitivity to dural and/or non-image forming retinal ganglion cell stimulation. However, it remains unclear if this light-aversive behavior is migraine-like or anxiety-like. To begin to answer this question, we asked if manipulation of the dPAG, a brain structure implicated in aversion and anxiety-related behaviors, would elicit similar results as the posterior thalamic manipulations. To investigate the role of the dPAG in light aversive behavior, we chose to target cell bodies of the dPAG for stimulation. We accomplished this using the pan-neuronal synapsin promoter to drive expression of ChR2 in neuronal cell bodies of the dPAG. Optical stimulation of the dPAG using the same stimulation protocol as the posterior thalamus decreased the time in light of ChR2-eYFP-expressing mice relative to eYFP controls (Fig. 5A, B). These experiments were performed at 2.7×10^4 lux to induce a maximal behavioral response. As in the case of posterior thalamic nuclei stimulation, there was no change in resting in light, but resting in the dark was increased in ChR2-eYFP mice compared to eYFP mice (Fig. 5C, D). However, in contrast to optical stimulation of the posterior thalamic nuclei, stimulation of the dPAG caused mice to spend less time in the center in the open field assay (Fig. 5E). This indicates that dPAG stimulation increased anxiety-like behavior, suggesting that the light-aversive behavior in this case may be due to increased anxiety [36]. The accuracy of targeting the dPAG was confirmed by histological identification of the eYFP reporter signal (Fig. 5F)

and the optical fiber tip locations (11/11 ChR2-eYFP fiber optic probe tips were on the most dorsal border of the PAG or directly dorsal in the superior colliculus).

Given that we saw a behavioral response with optical stimulation of cell bodies in the dPAG, we asked what role CGRP could be playing in the same area. The mice were tested at 55 lux similar to the CGRP conditions following posterior thalamic injections. CGRP (1 μg) was injected into the right dPAG, which resulted in no change to light-aversive behaviors (Fig. 6A-D). There was also no change in the open field behavior (Fig. 6E). To minimize diffusion into the vPAG, the injections were done at the extreme dorsal region, which likely resulted in some diffusion into the nearby superior colliculus. Correct targeting of injections was confirmed by injections of red beads (10 mice with 10/10 in the dPAG) (data not shown) and Evans blue dye injection in subsets of mice that were not used for behavioral studies (Fig. 6F).

The dorsal hippocampus does not contribute to light-aversive behavior in response to optical stimulation or CGRP injection

It was important to discount the possibility that perturbation of any brain region containing CGRP or its receptors could change light-aversive behaviors. The dorsal hippocampus was used as a control because of its proximity to the posterior thalamus and because it contains CGRP and CGRP receptor components, yet was not expected to be directly involved in light-aversive behavior [25, 26]. Optogenetic stimulation of mice expressing ChR2-eYFP driven by the CaMKIIa promoter in the dorsal hippocampus did not affect any of these behaviors (Fig. 7A-F). Injection targets are shown in figures 7F with 11/11 fiber optic probe tips correctly placed in the hippocampus or just dorsal to the hippocampus. Like with posterior thalamic nuclei and dPAG stimulation, we used the bright light stimulus for the dorsal hippocampus. Similarly, CGRP (1μg) injection into the hippocampus did not affect light-aversive behavior, resting or open field behavior (Fig. 8A-E). Targeting is indicated in Fig. 8F. As with the posterior thalamic region, 55 lux was used with the hippocampal CGRP injections. These data demonstrate that stimulation by ChR2 or injection of CGRP does not trigger light-aversive, resting, or anxiety-like behaviors in the hippocampus.

Discussion

Although photophobia is a complex behavior that likely involves multiple brain regions [37], the results of this study suggest that activation of the posterior thalamus is sufficient to induce light-aversive behaviors. Both optogenetic stimulation and injection of CGRP led to increased light aversion in mice without causing an anxiety-like phenotype. The behavior elicited by optical stimulation of posterior thalamic nuclei closely matched the CGRP-induced phenotype. This was not a general response of perturbing the CNS since the same manipulations in the dorsal hippocampus had no effect. Furthermore, optogenetic stimulation of the dPAG caused light aversion that was accompanied by an anxiogenic response, consistent with other reports [23, 24], and CGRP had no effect in the dPAG. Within the posterior thalamic nuclei, fiber optic tips were primarily located in the PO (51%) and LP (38%), suggesting that these regions are sufficient to induce light-aversive behavior. Likewise, CGRP binding was prevalent in the PO and medial regions of the posterior

thalamus. However, there was extensive spread throughout the posterior thalamic region (including nuclei outside of the posterior thalamus) of fluoro-15-CGRP. Therefore, it is difficult to pinpoint which regions of the posterior thalamic region are critical for the CGRP response and future studies will concentrate on pinpointing these regions. Combined, these data do suggest that both optical stimulation and CGRP may be acting on similar circuitry within the posterior thalamus, given their similar behavioral results. While recent clinical evidence strongly points to a peripheral site of CGRP action in migraine [8, 38], many preclinical studies suggest that CGRP in the CNS also contributes to the neural symptoms of migraine [4, 39–41]. In this regard, the shared phenotype of CGRP-induced light aversion following injection into the posterior thalamus with either injection into ventricles [11, 13] or the peritoneum [12] suggests that nuclei within the posterior thalamus may integrate central and peripheral signals to cause migraine-like photophobia.

What might CGRP be doing in the posterior thalamic region? While speculative, CGRP might increase glutamatergic signaling. This was the rationale for using the CaMKIIa promoter to drive optical stimulation because it should preferentially drive expression in glutamatergic neurons of the thalamus, including posterior thalamic nuclei [30]. A neuromodulatory role for CGRP is based on its known ability to act both presynaptically to increase glutamate release and postsynaptically to increase AMPA and NMDA receptors [42–45]. CGRP enhanced glutamatergic neurotransmission has been reported in the thalamus, amygdala, cingulate and insular cortex, and spinal cord dorsal horn [17, 42–45]. Indeed, there is robust staining of the glutamatergic marker VGluT2 in fibers in the posterior thalamus [32]. Furthermore, excitatory glutamatergic neurons in the posterior thalamus project to cortical areas [46]. In particular, the somatosensory cortex receives nociceptive input from the thalamus, including fibers from light and dural responsive neurons [14]. Finally, another study suggesting that blockade of CGRP receptors in the VPM alters glutamate-induced or sagittal sinus stimulation induced thalamic neuronal firing, further suggesting that CGRP enhances glutamatergic signaling in posterior thalamic nuclei [17]. While this last study suggests there is postsynaptic activity of CGRP in the posterior thalamic nuclei, presynaptic activity cannot be ruled out. The effect of CGRP on the network in the posterior thalamic nuclei is interesting since we are performing our behavior experiments 1h post injection, well past the expected half-life of CGRP. However, CGRP half life has not been determined in the cerebral spinal fluid and could be substantially longer than in the plasma where it is 6.9 minutes [47]. If the CGRP is rapidly degraded in the cerebral spinal fluid, it is likely that CGRP is sensitizing the network in that region to increase sensory input including light.

Moreover, a caveat of the current study is that we have not defined which neurons ChR2 is expressed in. While we propose that it is likely glutamatergic neurons, future studies are needed to define the specific populations of neurons responsible for these behavior responses. Nonetheless, increased pre or postsynaptic CGRP signaling in posterior thalamic nuclei could tip the balance between normal sensory perception and a hypersensitive state. In this regard, immunohistochemical staining revealed a diffuse CGRP fiber network in the posterior thalamic region. In addition, CGRP immunoreactive fibers have been reported in two nuclei near the posterior thalamus, the intralaminar thalamic and subparafasicular thalamic nuclei, which is intriguing because these nuclei receive somatosensory and nociceptive stimuli from ascending pain pathways [48]. These two nuclei are close to the

posterior thalamic injection sites and the CL nucleus of the intralaminar thalamus is within the targeted area. Furthermore, convergence of auditory and nociceptive inputs in one of these nuclei, the subparafasicular thalamic nucleus (ventral to the posterior thalamic nuclei), is important for conditioned auditory and visual fear responses [49, 50]. This is consistent with reports that neurons in posterior thalamic nuclei respond to CGRP and its antagonists [17]. However, Noseda et al., showed that neurons of the posterior thalamic nuclei that are sensitive to both light and dural stimulation were not near fibers positive for CGRP [32]. These observations can be reconciled by CGRP acting via volume transmission, diffusing from a relatively distant site to act on the dural/light-sensitive neurons rather than directly on synaptic connections [51]. Moreover, the relatively sparse innervation of the posterior thalamic nuclei by CGRP fibers relative to other areas, such as the central nucleus of the amygdala, suggests that a relatively small increase in CGRP release could have a large modulatory effect. Thus, the results of this study and of Burstein and colleagues [14] point to the posterior thalamic nuclei as an integration center for light aversion. This is consistent with other studies implicating regions in and near the posterior thalamic region in hypersensitivity aversion responses to somatosensory, auditory, and nociceptive stimuli [48–50]. However, the posterior thalamic nuclei are clearly not the only integrative regions of light and pain circuitry [52].

A caveat of this study is that the exact location of CGRP action within the posterior thalamic region and elsewhere was not resolved due to the broad diffusion of the peptide. Injection of fluorescent CGRP showed diffusion of at least 1400 μm, which is consistent with the ability of other peptides to diffuse up to millimeters in the brain [35]. Importantly, in addition to showing the likely diffusion range, the fluorescent CGRP also revealed several clusters of neurons within the posterior thalamus that bind CGRP, especially in the PO, just dorsal to the medial dorsal nucleus of the thalamus lateral part (MDL), and in the lateral habenula (LH). Furthermore, while there was a large diffusion range, diffusion into the cerebrospinal fluid and to a more distant target can be ruled out. This conclusion is based on posterior thalamic injections of CGRP causing light aversion in wild-type mice in dim light, which was not seen after ICV injections of CGRP [10]. For the dPAG injections, a caveat is that the lack of detectable CGRP effects may be confounded by contributions from the nearby superior colliculus, which has CGRP fibers [53] and receptors [54].

A feature of photophobia that has intrigued the migraine community is that patients are sensitive even to dim light. An unexpected finding of this study is that wild-type mice were sensitive to dim light following CGRP injection or optogenetic stimulation of posterior thalamic nuclei. This is in contrast to ICV injection of CGRP, which caused wild-type mice to choose the dark chamber only in bright light equivalent to a sunny day and required pre-exposure to the chamber to reduce exploratory drive [10, 12]. Sensitivity to dim light had only been observed in transgenic mice expressing elevated levels of CGRP receptor components in the nervous system [10–12], suggesting that heightened sensitivity to light required heightened sensitivity to CGRP. By direct administration to the posterior thalamic region, the requirement for increased CGRP receptors appears to have been bypassed, presumably because the local concentration of CGRP was greater than after ICV injection. Furthermore, the fact that the results from optical stimulation of posterior thalamic nuclei in bright light were indistinguishable from those in dim light suggests that dim and bright light trigger

light-aversive behaviors via similar pathways in the brain downstream of retinal input. Within the eye, in dim light (55 lux) it is likely that rods and cones, but not melanopsin-containing cells are active. While in bright light (2.7×10^4 lux), it is likely that the rods are bleached so that only cones and melanopsin-containing cells are responding at this brightness level. Therefore, at low lights intensities, it is possible that the stimuli is rod-driven as was recently reported in humans [55], and in bright light it could be cone and melanopsin-driven light aversion. It should be noted that it seems unlikely that aversion to bright light is a protective mechanism against retinal damage since both C57BL6/J and CD1 mice spend similar amounts of time in dim or bright light in the absence of CGRP [10, 12, 56].

One interesting observation of this study is that optical stimulation of the dPAG also induced light-aversive behavior. These results are consistent with the role of the dPAG in aversion and anxiety-like behaviors and indeed, the increased light aversion induced by dPAG optical stimulation was accompanied by anxiety-like behavior in open field. These results are also consistent with observed PAG projections to the superior salivatory nucleus, which can regulate autonomic responses such as anxiety [57]. These same PAG neurons also receive input from retinal ganglion cells, thus possibly positioning those neurons to integrate autonomic and light responses [57]. Interestingly, CGRP injection in the dPAG had no effect on light-aversive or open field behaviors suggesting that CGRP does not directly play a role in light-aversive or anxiety-like behaviors generated by the dPAG. In contrast, Pozo-Rasich et al., demonstrated that CGRP injection into the ventrolateral PAG modulates activity of neurons in the trigeminal cervical complex [58]. Together, with the optical stimulation and CGRP injection data in the posterior thalmus, the dPAG data support the idea that posterior thalamic nuclei-induced light-aversion is consistent with migraine-like behavior while the dPAG behavior is consistent with anxiety-related aversion.

Within the posterior thalamic nuclei, where might the CGRP inputs come from and project to? Future studies should consider the parabrachial nucleus (PBN) as a potential input source of CGRP. Glutamatergic CGRP-containing neurons in the PBN that project to the amygdala contribute to aversive behaviors and pain [59]. While speculative, the presence of PBN projections to the VPMpc of the posterior thalamic nuclei [60] raises the possibility that they contribute to light-aversive behavior. Conversely, where do the posterior thalamic nuclei neurons that contribute to light aversion project to? Two likely sites are the somatosensory and visual cortices, which are known to receive input from posterior thalamic nuclei [14]. Indeed, eYFP-positive neurons were found to project from the posterior thalamic nuclei to the somatosensory cortex. Further studies are needed to identify the sites from which CGRP-containing fibers in the posterior thalamic nuclei originate, as well as the targets to which those neurons project to cause light-aversive behavior.

Conclusion

In conclusion, this study reveals that stimulation of posterior thalamic nuclei is sufficient to induce light-aversive behavior in mice. Further, the data suggest that central CGRP signaling in this region contributes to light-aversive behavior. Since current CGRP blocking drugs preferentially work in the periphery and only work in about 50% of patients, it is possible that central sites of CGRP action may represent a new therapeutic target for migraine.

Acknowledgments

Funding: This work was supported by grants from the NIH (NS075599) and Department of Veterans Affairs to AFR (1I01RX002101) and LPS (IK2 RX-002010-01). JAW is supported by VA Merit Review (IO1BX004440) and NIMH (R01 MH113325). The contents do not represent the views of VA or the United States Government.

References Cited

1. GBD. Global, regional, and national burden of migraine and tension-type headache, 1990–2016: a systematic analysis for the Global Burden of Disease Study 2016. Lancet Neurol 2018; 17: 954–976. 2018/10/26. DOI: 10.1016/S1474-4422(18)30322-3. [PubMed: 30353868]
2. de Tommaso M, Ambrosini A, Brighina F, et al. Altered processing of sensory stimuli in patients with migraine. Nat Rev Neurol 2014; 10: 144–155. 2014/02/19. DOI: 10.1038/nrneurol.2014.14. [PubMed: 24535465]
3. Noseda R and Burstein R. Advances in understanding the mechanisms of migraine-type photophobia. Curr Opin Neurol 2011; 24: 197–202. 2011/04/07. DOI: 10.1097/WCO.0b013e3283466c8e. [PubMed: 21467933]
4. Russo AF. Calcitonin gene-related peptide (CGRP): a new target for migraine. Annu Rev Pharmacol Toxicol 2015; 55: 533–552. 2014/10/24. DOI: 10.1146/annurev-pharmtox-010814-124701. [PubMed: 25340934]
5. Russell FA, King R, Smillie SJ, et al. Calcitonin gene-related peptide: physiology and pathophysiology. Physiol Rev 2014; 94: 1099–1142. 2014/10/08. DOI: 10.1152/physrev.00034.2013. [PubMed: 25287861]
6. Ho TW, Edvinsson L and Goadsby PJ. CGRP and its receptors provide new insights into migraine pathophysiology. Nat Rev Neurol 2010; 6: 573–582. 2010/09/08. DOI: 10.1038/nrneurol.2010.127. [PubMed: 20820195]
7. Wattiez AS, Sowers LP and Russo AF. Calcitonin gene-related peptide (CGRP): role in migraine pathophysiology and therapeutic targeting. Expert Opin Ther Targets 2020; 24: 91–100. 2020/02/01. DOI: 10.1080/14728222.2020.1724285. [PubMed: 32003253]
8. Russo AF. CGRP-Based MIgraine Therapeutics: How Might They Work, Why So Safe, and What Next?. ACS Pharmacology and Translational Science 2019; 2: 2–8. [PubMed: 31559394]
9. Edvinsson L, Haanes KA, Warfvinge K, et al. CGRP as the target of new migraine therapies - successful translation from bench to clinic. Nat Rev Neurol 2018; 14: 338–350. 2018/04/25. DOI: 10.1038/s41582-018-0003-1. [PubMed: 29691490]
10. Kaiser EA, Kuburas A, Recober A, et al. Modulation of CGRP-induced light aversion in wild-type mice by a 5-HT(1B/D) agonist. J Neurosci 2012; 32: 15439–15449. 2012/11/02. DOI: 10.1523/JNEUROSCI.3265-12.2012. [PubMed: 23115181]
11. Recober A, Kaiser EA, Kuburas A, et al. Induction of multiple photophobic behaviors in a transgenic mouse sensitized to CGRP. Neuropharmacology 2010; 58: 156–165. 2009/07/18. DOI: 10.1016/j.neuropharm.2009.07.009. [PubMed: 19607849]
12. Mason BN, Kaiser EA, Kuburas A, et al. Induction of Migraine-Like Photophobic Behavior in Mice by Both Peripheral and Central CGRP Mechanisms. J Neurosci 2017; 37: 204–216. 2017/01/06. DOI: 10.1523/JNEUROSCI.2967-16.2016. [PubMed: 28053042]
13. Recober A, Kuburas A, Zhang Z, et al. Role of calcitonin gene-related peptide in light-aversive behavior: implications for migraine. J Neurosci 2009; 29: 8798–8804. 2009/07/10. DOI: 10.1523/JNEUROSCI.1727-09.2009. [PubMed: 19587287]
14. Noseda R, Kainz V, Jakubowski M, et al. A neural mechanism for exacerbation of headache by light. Nat Neurosci 2010; 13: 239–245. 2010/01/12. DOI: 10.1038/nn.2475. [PubMed: 20062053]
15. Maleki N, Becerra L, Upadhyay J, et al. Direct optic nerve pulvinar connections defined by diffusion MR tractography in humans: implications for photophobia. Hum Brain Mapp 2012; 33: 75–88. 2011/02/22. DOI: 10.1002/hbm.21194. [PubMed: 21337474]
16. Delwig A, Logan AM, Copenhagen DR, et al. Light evokes melanopsin-dependent vocalization and neural activation associated with aversive experience in neonatal mice. PLoS One 2012; 7: e43787 2012/10/03. DOI: 10.1371/journal.pone.0043787. [PubMed: 23028470]

17. Summ O, Charbit AR, Andreou AP, et al. Modulation of nocioceptive transmission with calcitonin gene-related peptide receptor antagonists in the thalamus. Brain 2010; 133: 2540–2548. 2010/08/31. DOI: 10.1093/brain/awq224. [PubMed: 20802202]

18. Afridi SK, Giffin NJ, Kaube H, et al. A positron emission tomographic study in spontaneous migraine. Arch Neurol 2005; 62: 1270–1275. 2005/08/10. DOI: 10.1001/archneur.62.8.1270. [PubMed: 16087768]

19. Yen CT and Lu PL. Thalamus and pain. Acta Anaesthesiol Taiwan 2013; 51: 73–80. 2013/08/24. DOI: 10.1016/j.aat.2013.06.011. [PubMed: 23968658]

20. Hudson AJ. Pain perception and response: central nervous system mechanisms. Can J Neurol Sci 2000; 27: 2–16. 2000/02/17.

21. Jia Z, Tang W, Zhao D, et al. Disrupted functional connectivity between the periaqueductal gray and other brain regions in a rat model of recurrent headache. Sci Rep 2017; 7: 3960 2017/06/24. DOI: 10.1038/s41598-017-04060-6. [PubMed: 28638117]

22. Welch KM, Nagesh V, Aurora SK, et al. Periaqueductal gray matter dysfunction in migraine: cause or the burden of illness? Headache 2001; 41: 629–637. 2001/09/14. [PubMed: 11554950]

23. Deng H, Xiao X and Wang Z. Periaqueductal Gray Neuronal Activities Underlie Different Aspects of Defensive Behaviors. J Neurosci 2016; 36: 7580–7588. 2016/07/23. DOI: 10.1523/JNEUROSCI.4425-15.2016. [PubMed: 27445137]

24. Evans DA, Stempel AV, Vale R, et al. A synaptic threshold mechanism for computing escape decisions. Nature 2018; 558: 590–594. 2018/06/22. DOI: 10.1038/s41586-018-0244-6. [PubMed: 29925954]

25. Skofitsch G and Jacobowitz DM. Calcitonin gene-related peptide: detailed immunohistochemical distribution in the central nervous system. Peptides 1985; 6: 721–745. 1985/07/01. [PubMed: 3906594]

26. Ueda T, Ugawa S, Saishin Y, et al. Expression of receptor-activity modifying protein (RAMP) mRNAs in the mouse brain. Brain Res Mol Brain Res 2001; 93: 36–45. 2001/09/05. [PubMed: 11532336]

27. Carter ME, Soden ME, Zweifel LS, et al. Genetic identification of a neural circuit that suppresses appetite. Nature 2013; 503: 111–114. 2013/10/15. DOI: 10.1038/nature12596. [PubMed: 24121436]

28. Lein ES, Hawrylycz MJ, Ao N, et al. Genome-wide atlas of gene expression in the adult mouse brain. Nature 2007; 445: 168–176. 2006/12/08. DOI: 10.1038/nature05453. [PubMed: 17151600]

29. Simms J, Uddin R, Sakmar TP, et al. Photoaffinity Cross-Linking and Unnatural Amino Acid Mutagenesis Reveal Insights into Calcitonin Gene-Related Peptide Binding to the Calcitonin Receptor-like Receptor/Receptor Activity-Modifying Protein 1 (CLR/RAMP1) Complex. Biochemistry 2018; 57: 4915–4922. 2018/07/14. DOI: 10.1021/acs.biochem.8b00502. [PubMed: 30004692]

30. Liu XB and Murray KD. Neuronal excitability and calcium/calmodulin-dependent protein kinase type II: location, location, location. Epilepsia 2012; 53 Suppl 1: 45–52. 2012/05/25. DOI: 10.1111/j.1528-1167.2012.03474.x.

31. Ashby R, Ohlendorf A and Schaeffel F. The effect of ambient illuminance on the development of deprivation myopia in chicks. Invest Ophthalmol Vis Sci 2009; 50: 5348–5354. 2009/06/12. DOI: 10.1167/iovs.09-3419. [PubMed: 19516016]

32. Noseda R, Kainz V, Borsook D, et al. Neurochemical pathways that converge on thalamic trigeminovascular neurons: potential substrate for modulation of migraine by sleep, food intake, stress and anxiety. PLoS One 2014; 9: e103929 2014/08/05. DOI: 10.1371/journal.pone.0103929. [PubMed: 25090640]

33. Kresse A, Jacobowitz DM and Skofitsch G. Detailed mapping of CGRP mRNA expression in the rat central nervous system: comparison with previous immunocytochemical findings. Brain Res Bull 1995; 36: 261–274. 1995/01/01. [PubMed: 7697380]

34. Kawai Y, Takami K, Shiosaka S, et al. Topographic localization of calcitonin gene-related peptide in the rat brain: an immunohistochemical analysis. Neuroscience 1985; 15: 747–763. 1985/07/01. [PubMed: 3877882]

35. van den Pol AN. Neuropeptide transmission in brain circuits. Neuron 2012; 76: 98–115. 2012/10/09. DOI: 10.1016/j.neuron.2012.09.014. [PubMed: 23040809]
36. Graeff FG, Silveira MC, Nogueira RL, et al. Role of the amygdala and periaqueductal gray in anxiety and panic. Behav Brain Res 1993; 58: 123–131. 1993/12/20. [PubMed: 8136040]
37. Noseda R, Copenhagen D and Burstein R. Current understanding of photophobia, visual networks and headaches. Cephalalgia 2018: 333102418784750 2018/06/27. DOI: 10.1177/0333102418784750.
38. Rujan RM and Reynolds CA. Calcitonin Gene-Related Peptide Antagonists and Therapeutic Antibodies. Handb Exp Pharmacol 2019 2019/01/29. DOI: 10.1007/164_2018_173.
39. Goadsby PJ, Lipton RB and Ferrari MD. Migraine--current understanding and treatment. N Engl J Med 2002; 346: 257–270. 2002/01/25. DOI: 10.1056/NEJMra010917. [PubMed: 11807151]
40. Messlinger K Migraine: where and how does the pain originate? Exp Brain Res 2009; 196: 179–193. 2009/03/17. DOI: 10.1007/s00221-009-1756-y. [PubMed: 19288089]
41. Pietrobon D and Striessnig J. Neurobiology of migraine. Nat Rev Neurosci 2003; 4: 386–398. 2003/05/03. DOI: 10.1038/nrn1102. [PubMed: 12728266]
42. Seybold VS. The role of peptides in central sensitization. Handb Exp Pharmacol 2009: 451–491. 2009/08/06. DOI: 10.1007/978-3-540-79090-7_13.
43. Han JS, Adwanikar H, Li Z, et al. Facilitation of synaptic transmission and pain responses by CGRP in the amygdala of normal rats. Mol Pain 2010; 6: 10 2010/02/11. DOI: 10.1186/1744-8069-6-10. [PubMed: 20144185]
44. Li XH, Matsuura T, Liu RH, et al. Calcitonin gene-related peptide potentiated the excitatory transmission and network propagation in the anterior cingulate cortex of adult mice. Mol Pain 2019; 15: 1744806919832718 2019/02/06. DOI: 10.1177/1744806919832718. [PubMed: 30717631]
45. Liu Y, Chen QY, Lee JH, et al. Cortical potentiation induced by calcitonin gene-related peptide (CGRP) in the insular cortex of adult mice. Mol Brain 2020; 13: 36 2020/03/11. DOI: 10.1186/s13041-020-00580-x. [PubMed: 32151282]
46. Kaneko T and Mizuno N. Immunohistochemical study of glutaminase-containing neurons in the cerebral cortex and thalamus of the rat. J Comp Neurol 1988; 267: 590–602. 1988/01/22. DOI: 10.1002/cne.902670411. [PubMed: 2450108]
47. Kraenzlin ME, Ch'ng JL, Mulderry PK, et al. Infusion of a novel peptide, calcitonin gene-related peptide (CGRP) in man. Pharmacokinetics and effects on gastric acid secretion and on gastrointestinal hormones. Regul Pept 1985; 10: 189–197. 1985/03/01. DOI: 10.1016/0167-0115(85)90013-8. [PubMed: 3922013]
48. de Lacalle S and Saper CB. Calcitonin gene-related peptide-like immunoreactivity marks putative visceral sensory pathways in human brain. Neuroscience 2000; 100: 115–130. 2000/09/21. [PubMed: 10996463]
49. Coolen LM, Veening JG, Petersen DW, et al. Parvocellular subparafascicular thalamic nucleus in the rat: anatomical and functional compartmentalization. J Comp Neurol 2003; 463: 117–131. 2003/06/20. DOI: 10.1002/cne.10740.
50. Coolen LM, Veening JG, Wells AB, et al. Afferent connections of the parvocellular subparafascicular thalamic nucleus in the rat: evidence for functional subdivisions. J Comp Neurol 2003; 463: 132–156. 2003/06/20. DOI: 10.1002/cne.10739. [PubMed: 12815752]
51. Russo AF. Overview of Neuropeptides: Awakening the Senses? 2017; 57: 37–46. DOI: 10.1111/head.13084.
52. Chen Q, Roeder Z, Li MH, et al. Optogenetic Evidence for a Direct Circuit Linking Nociceptive Transmission through the Parabrachial Complex with Pain-Modulating Neurons of the Rostral Ventromedial Medulla (RVM). eNeuro 2017; 4 2017/07/01. DOI: 10.1523/ENEURO.0202-17.2017.
53. Gerrikagoitia I, Garcia del Cano G, Canudas J, et al. Expression pattern of calcitonin gene-related peptide in the superior colliculus during postnatal development: demonstration of its intrinsic nature and possible roles. J Comp Neurol 2006; 494: 721–737. 2005/12/24. DOI: 10.1002/cne.20834. [PubMed: 16374811]

54. Van Rossum D, Menard DP, Fournier A, et al. Binding profile of a selective calcitonin gene-related peptide (CGRP) receptor antagonist ligand, [125I-Tyr]hCGRP8–37, in rat brain and peripheral tissues. J Pharmacol Exp Ther 1994; 269: 846–853. 1994/05/01. [PubMed: 8182554]

55. Bernstein CA, Nir RR, Noseda R, et al. The migraine eye: distinct rod-driven retinal pathways' response to dim light challenges the visual cortex hyperexcitability theory. Pain 2019; 160: 569–578. 2018/10/31. DOI: 10.1097/j.pain.0000000000001434. [PubMed: 30376534]

56. Kuburas A, Thompson S, Artemyev NO, et al. Photophobia and abnormally sustained pupil responses in a mouse model of bradyopsia. Invest Ophthalmol Vis Sci 2014; 55: 6878–6885. 2014/09/27. DOI: 10.1167/iovs.14-14784. [PubMed: 25257059]

57. Noseda R, Lee AJ, Nir RR, et al. Neural mechanism for hypothalamic-mediated autonomic responses to light during migraine. Proc Natl Acad Sci U S A 2017; 114: E5683–E5692. 2017/06/28. DOI: 10.1073/pnas.1708361114. [PubMed: 28652355]

58. Pozo-Rosich P, Storer RJ, Charbit AR, et al. Periaqueductal gray calcitonin gene-related peptide modulates trigeminovascular neurons. Cephalalgia 2015; 35: 1298–1307. 2015/03/21. DOI: 10.1177/0333102415576723. [PubMed: 25792688]

59. Palmiter RD. The Parabrachial Nucleus: CGRP Neurons Function as a General Alarm. Trends Neurosci 2018; 41: 280–293. 2018/04/29. DOI: 10.1016/j.tins.2018.03.007. [PubMed: 29703377]

60. Chen JY, Campos CA, Jarvie BC, et al. Parabrachial CGRP Neurons Establish and Sustain Aversive Taste Memories. Neuron 2018; 100: 891–899 e895. 2018/10/23. DOI: 10.1016/j.neuron.2018.09.032. [PubMed: 30344042]

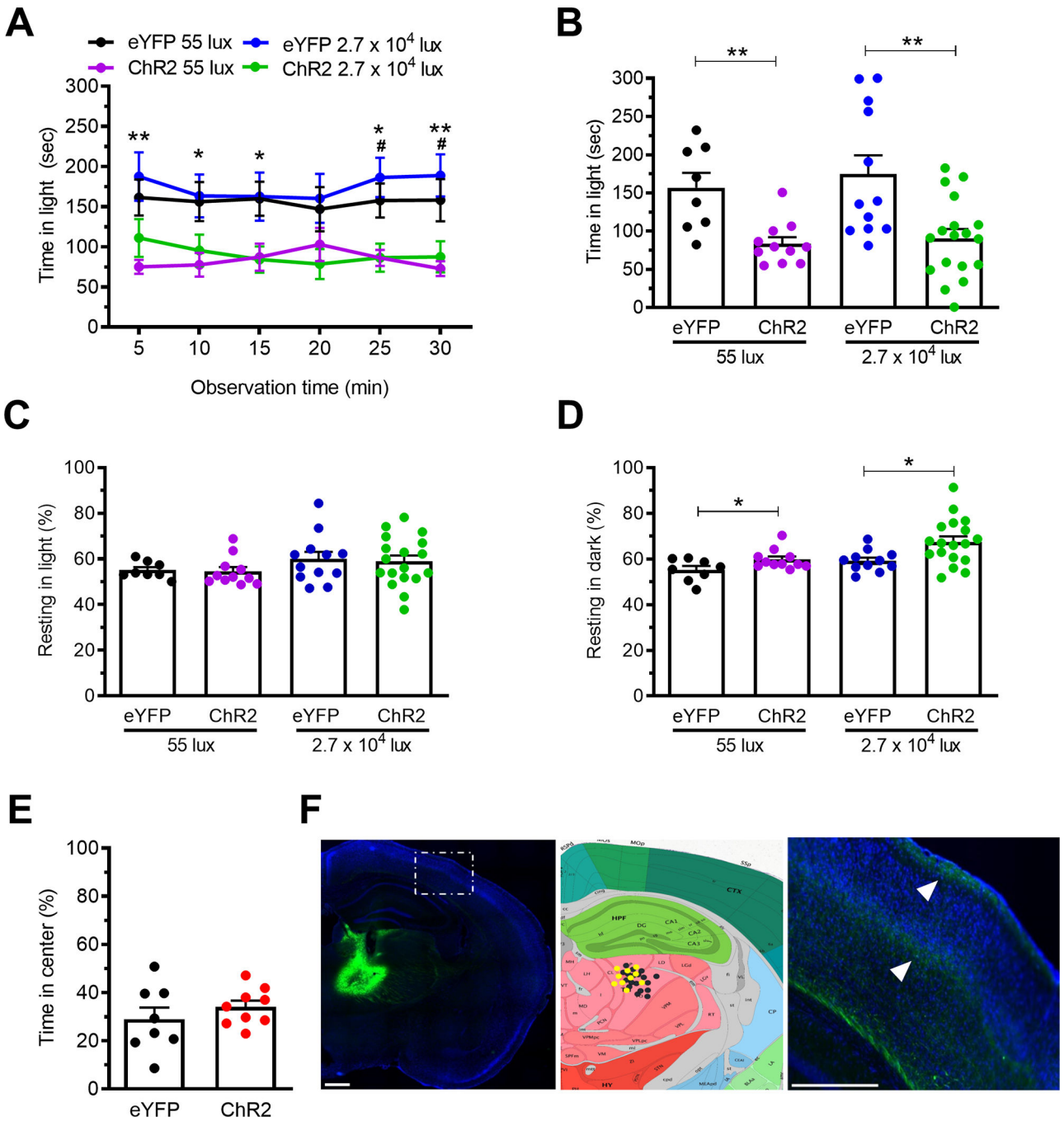

Figure 1. Optical stimulation of posterior thalamic nuclei induces light aversion in both dim and bright light.

A. Time in light during 30 min light/dark assay following optical stimulation of C57BL/6J mice injected with AAV encoding either ChR2 or eYFP (control). Light/dark testing was performed with different cohorts of mice at 55 lux (dim light) and 2.7×10^4 lux (bright light). All mice in panel A are further analyzed in panels B, C, D. **B.** Mean time in light per 5 min block of individual mice from panel A. **C.** Time resting in light during the assay. **D.** Time resting in dark during the assay. **E.** Time in center during open field assay. **F.** Left:

expression of AAV2-CaMKIIa-eYFP (green) in the posterior thalamic nuclei, counter stained with DAPI (blue). Middle: schematic of positions of optical fiber probe tips for all ChR2 mice. Mice tested at 55 lux are indicated in yellow and at 2.7×10^4 lux are in black symbols superimposed on Allen Mouse Brain Atlas coronal image (image 74/132). Image credit: Allen Institute. Right: magnified view of left-hand panel (dashed box) showing green axonal projections (arrowheads) from the posterior thalamic nuclei to the somatosensory cortex. Scale bar = 500 μm. All error bars are SEM, * $p < 0.05$, ** $p < 0.01$, $^{\#}$ $p < 0.05$, $^{\#\#}$ $p < 0.01$. See Table 1 for detailed statistical analyses. A-D: At 55 lux: eYFP n=8, ChR2 n=11; At 2.7×10^4 lux: eYFP n=12, ChR2 n=18. E: eYFP n=8, ChR2 n=9

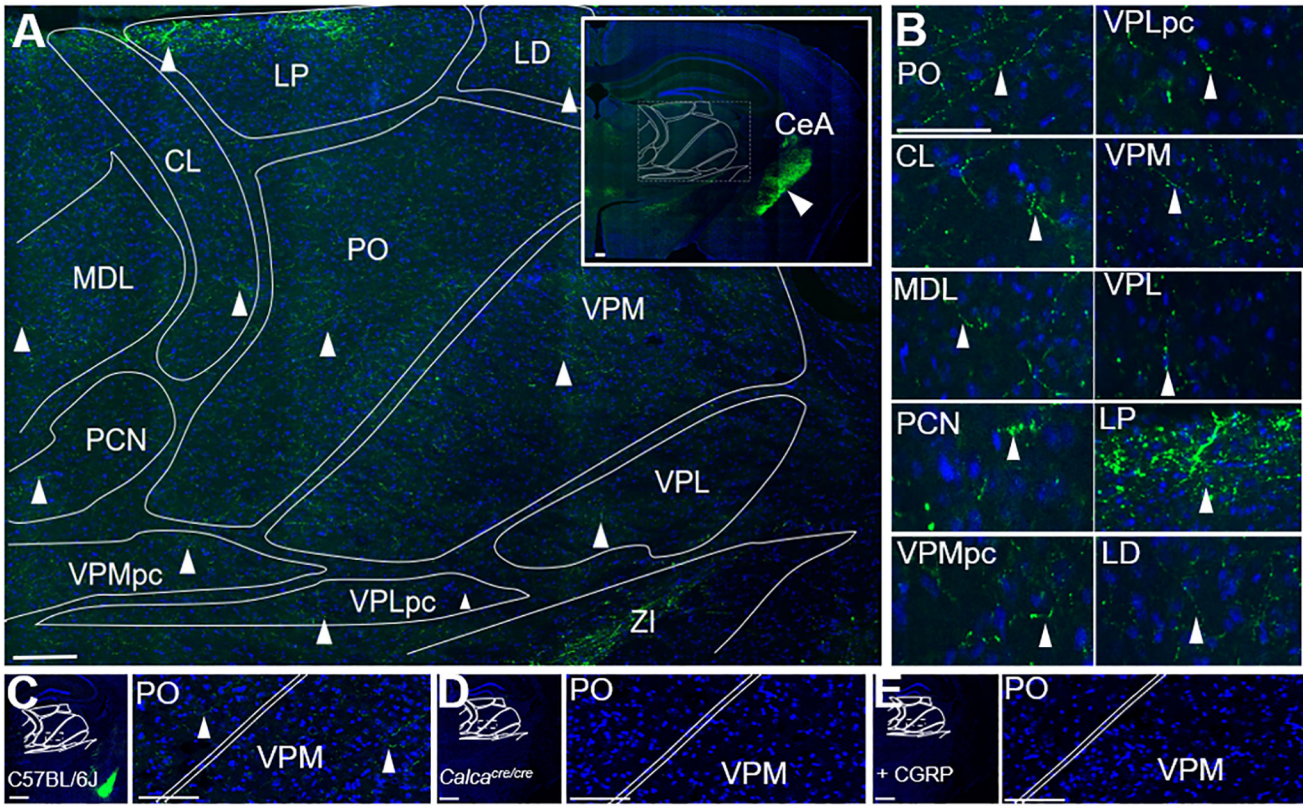

Figure 2. CGRP fibers are present in multiple nuclei of the posterior thalamus.

A. CGRP (green) staining of a C57BL/6J mouse coronal brain section counterstained with DAPI (blue). **B.** Magnified images of nuclei shown in panel A, with arrowheads highlighting CGRP-containing fibers. **C.** CGRP (green) staining of a C57BL/6J mouse coronal brain section counterstained with DAPI (blue) for comparison with controls in panels D and E. The bright amygdala signal can be seen in the lower right quadrant. Right panel is a magnified view of box in the left panel, CGRP-containing fibers indicated with arrowheads. **D.** CGRP staining of a *Calca*$^{cre/cre}$ mouse (which does not express αCGRP) coronal brain section, showing absence of staining. Right panel is a magnified view of box in left panel. **E.** CGRP staining C57BL/6J mouse coronal brain section after the primary antibody was pre-incubated with CGRP (20 μM), showing absence of staining. Right panel is magnified view of box in left panel. Abbreviations are: CL = central lateral nucleus of the thalamus, LD = lateral dorsal nucleus of the thalamus, LP = lateral posterior nucleus of the thalamus, PO = posterior thalamus, VPMpc = ventral posteromedial nucleus of the thalamus, parvicellular part, VPLpc = ventral posterolateral nucleus of the thalamus, parvicellular part, VPM = ventral posteromedial nucleus of the thalamus, VPL = ventral posterolateral nucleus of the thalamus. MDL = medial dorsal nucleus of the thalamus, PCN = paracentral nucleus, ZI = zona incerta. Scale bar = 100 μm for all images.

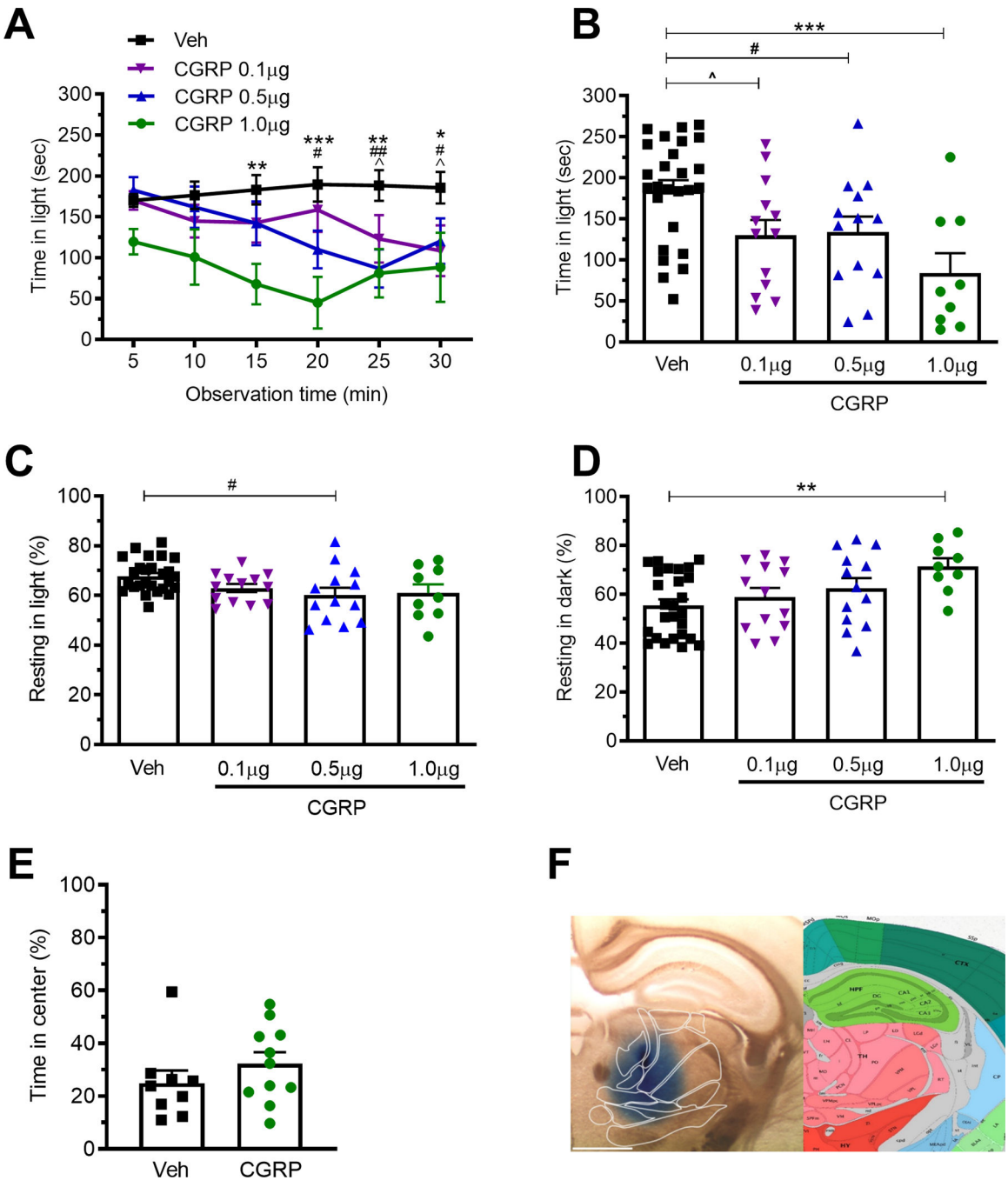

Figure 3. Injection of CGRP into the posterior thalamic region induces light-aversive behavior in dim light.

A. Time in light during 30 min light/dark assay following unilateral stereotactic injection of vehicle (Veh) or 0.1, 0.5, or 1.0 µg CGRP into the right posterior thalamic region of C57BL/6J mice. Light/dark testing was performed at 55 lux (dim light). All mice in panel A are further analyzed in panels B, C, D. **B.** Mean time in light per 5 min block of individual mice from panel A. **C.** Time resting in light during the assay. **D.** Time resting in dark during the assay. **E**. Time in center during the open field assay. **F.** Left: Site of injection of Evans

blue dye. Right: Allen Mouse Brain Atlas coronal image representative of the injected area (image 74/132). Image credit: Allen Institute. Scale bar = 1000 μm. All error bars are SEM, * $p < 0.05$, ** $p < 0.01$, *** $P<0.001$. # $p < 0.05$, ## $p < 0.01$, ^ $p < 0.05$. See Table 1 for detailed statistical analyses. A-D: Veh n=26, CGRP 1.0 μg n=9, 0.5 μg n=13, 0.1 μg n=13. E: Veh n=9, CGRP n=11.

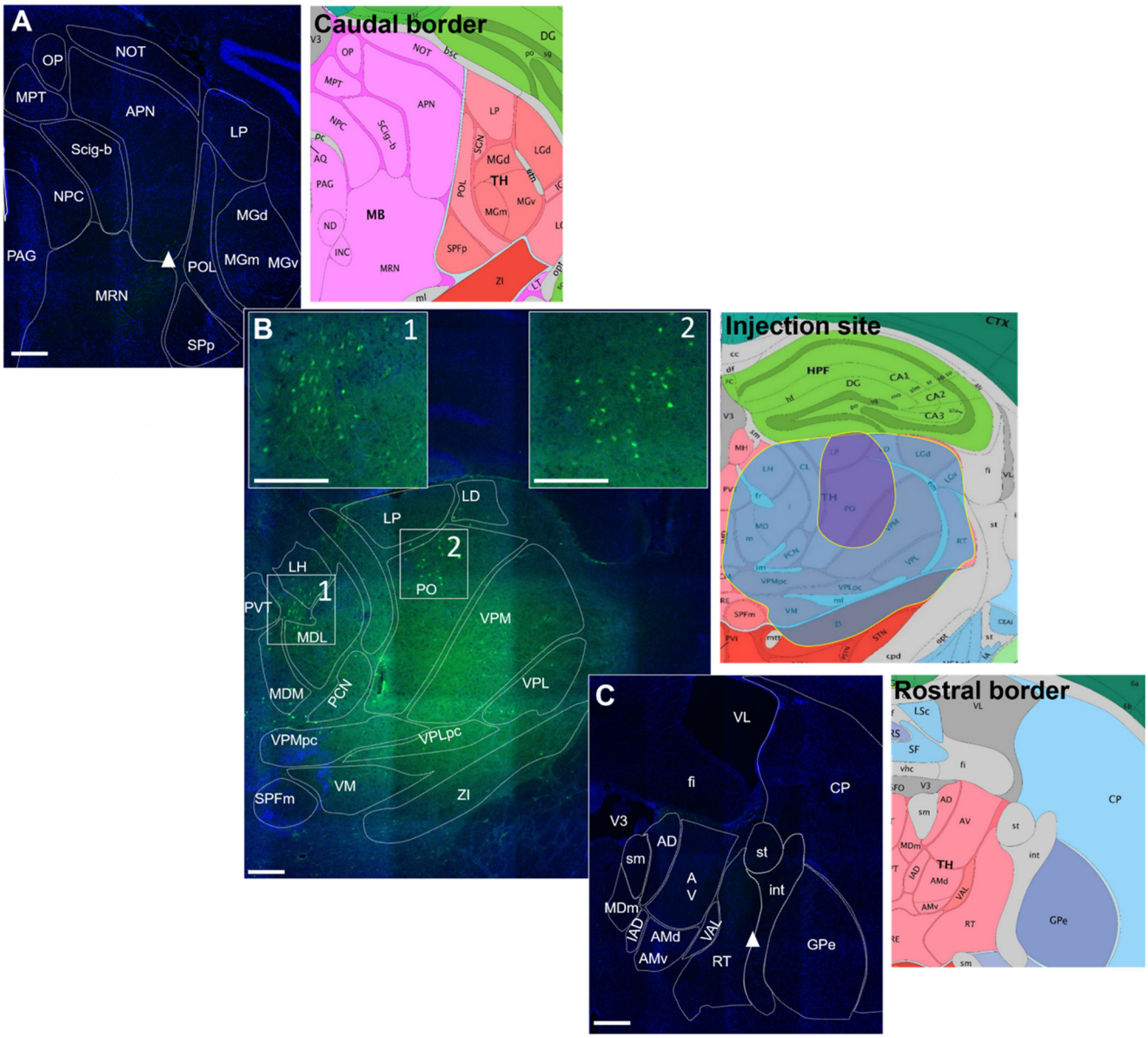

Figure 4. Fluoro-15-CGRP injection site targeting.

A. Caudal border of detectable signal from fluoro-15-CGRP (green) staining of a C57BL/6J mouse coronal brain section counterstained with DAPI (blue). Right panel is the Allen Mouse Brain Atlas coronal image representative of the brain slice (image 86/132). **B.** Fluoro-15-CGRP (1 μg) at the injection site. Boxes 1 and 2 represent magnified insets showing clusters of neurons that appear to have accumulated fluoro-15-CGRP signal. Right panel is the Allen Mouse Brain Atlas coronal image representative of the brain slice (image 74/132). The largest (blue shading) and smallest (purple shading) spread of the signal among the 5 mice are indicated. Shown here is the largest spread of the injections performed. **C.** Rostral border of detectable signal. Right panel is the representative Allen Mouse Brain Atlas coronal image (image 60/132). Image credit: Allen Institute. Scale bar = 100 μm for all images.

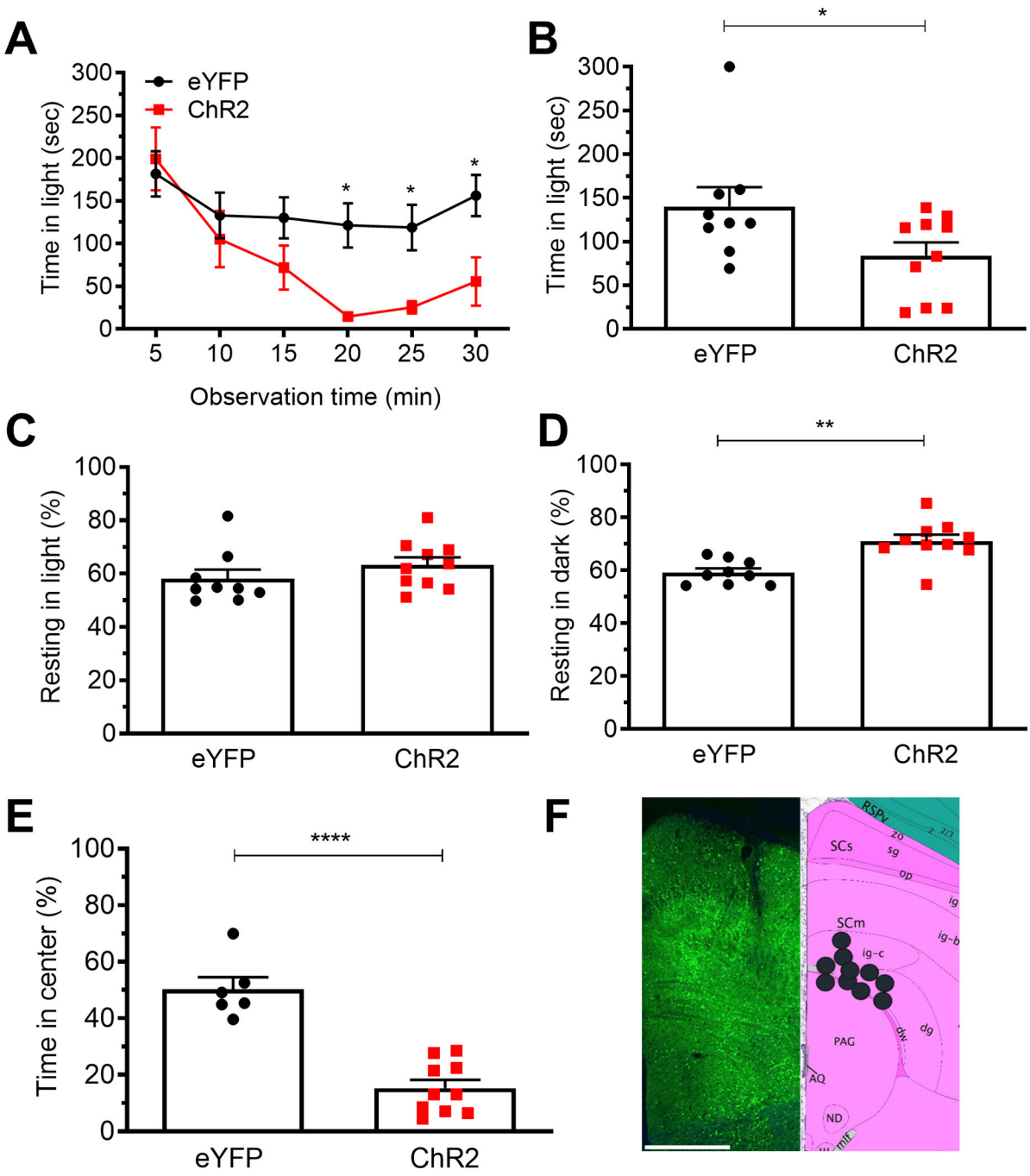

Figure 5. Optical stimulation of the dPAG induces light-aversive behavior accompanied by increased anxiety-like behavior.

A. Time in light over a 30 min light/dark assay in mice injected with AAV encoding either ChR2 or eYFP control in the dPAG. All mice in panel A are further analyzed in panels B, C, D. **B.** Mean time in light per 5 min block of individual mice from panel A. **C.** Time resting in light during the assay. **D.** Time resting dark during the assay. **E.** Time in center during the open field assay. **F.** Left: expression of AAV2-CaMKIIa-ChR2-eYFP in the dPAG. Right: schematic of positions of fiber optic probe tips for dPAG mice superimposed on Allen

Mouse Brain Atlas coronal image (image 90/132). Image credit: Allen Institute. Scale bar = 500 μm. All error bars are SEM, * $p < 0.05$, ** $p < 0.01$, **** $p < 0.001$. See Table 1 for detailed statistical analyses. A-D: eYFP n=9, ChR2 n=10. E: eYFP n=6, ChR2 n=10.

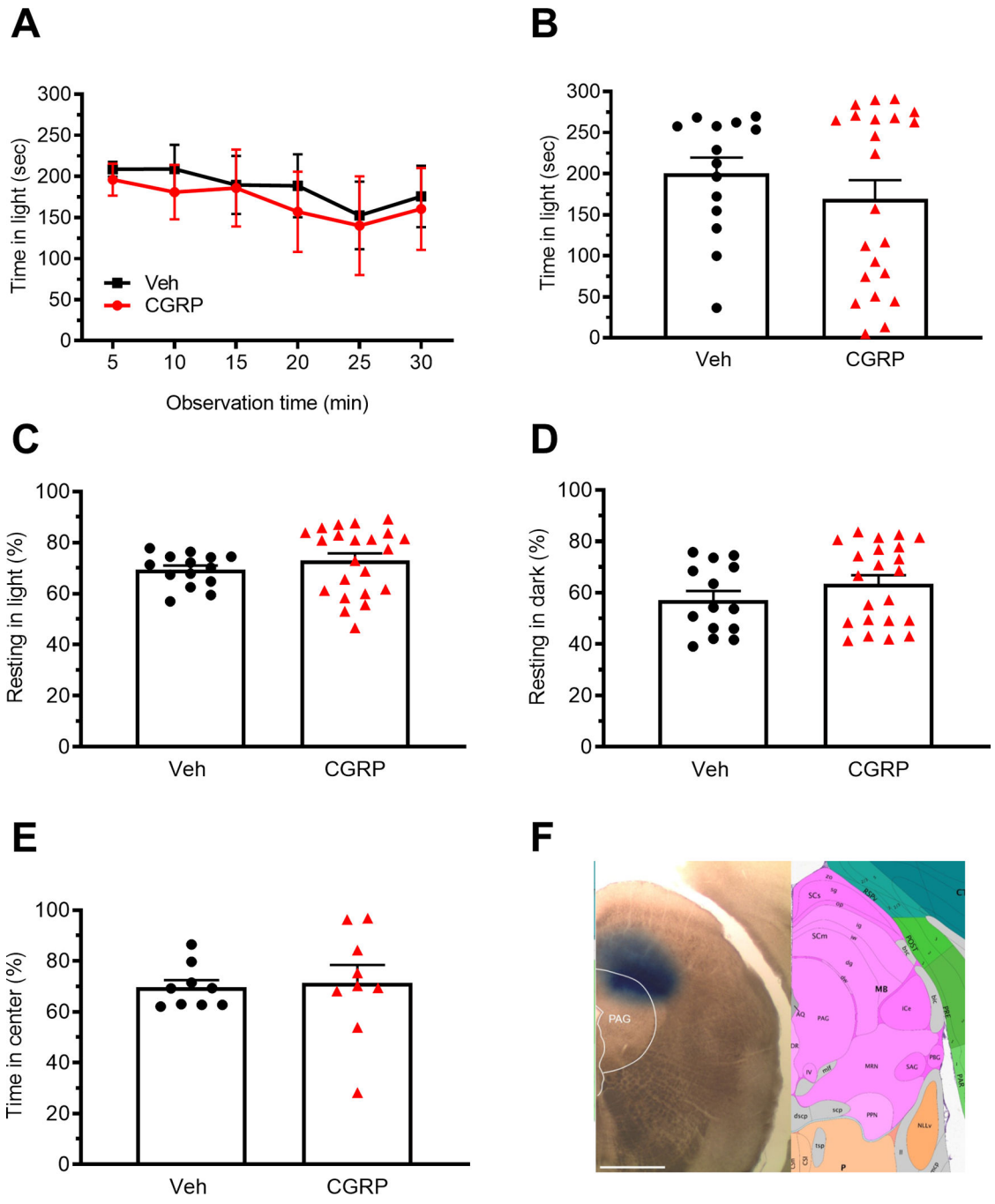

Figure 6. Injection of CGRP into the dPAG does not induce light-aversive behavior.

A. Time in light over a 30 min light/dark assay following unilateral CGRP injection into the dPAG. All mice in panel A are further analyzed in panels B, C, D. **B.** Mean time in light per 5 min interval of individual mice from panel A. **C.** Time resting in light during the assay. **D.** Time resting in dark during the assay. **E.** Time in center during the open field assay. **F.** Left: site of injection of Evans blue dye. Right: Allen Mouse Brain Atlas coronal image (image 90/132) representative of injected area. Image credit: Allen Institute. Scale bar = 1000 μm.

All error bars are SEM. No statistical analyses performed on these data were significantly different (see Table 1). A-D: Veh n=14, CGRP n=22. E: Veh n=9, CGRP n=9.

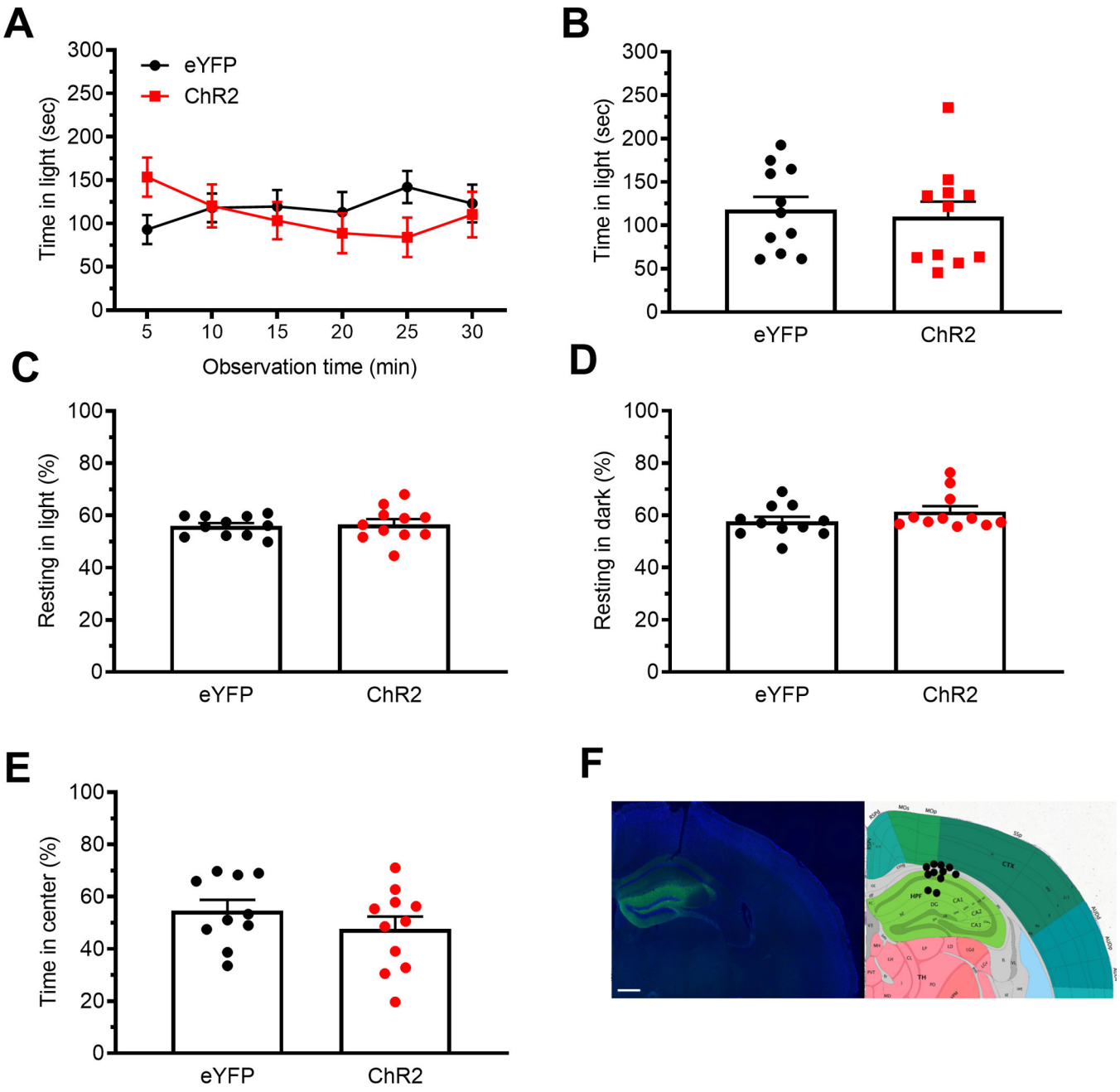

Figure 7. Optical stimulation of the dorsal hippocampus does not induce light-aversive behavior.

A. Time in light over a 30 min light/dark assay in mice injected with AAV encoding either ChR2 or eYFP control were stimulated. All mice in panel A are further analyzed in panels B, C, D. **B.** Mean time in light per 5 min block of individual mice from panel A. **C.** Time resting in light during the assay. **D.** Time resting in dark during the assay. **E.** Time spent in center in the open field assay. **F.** Left: expression of AAV2-CaMKIIa-ChR2-eYFP in the dorsal hippocampus with DAPI counterstain. Right: schematic of positions of fiber optic probe tips for the dorsal hippocampus superimposed on Allen Mouse Brain Atlas coronal image (image 74/132). Image credit: Allen Institute. Scale bar = 500 μm. All error bars are

SEM. No statistical analyses performed on these data were significantly different (see Table 1). A-D: eYFP n=11, ChR2 n=11. E: eYFP n=10, ChR2 n=11.

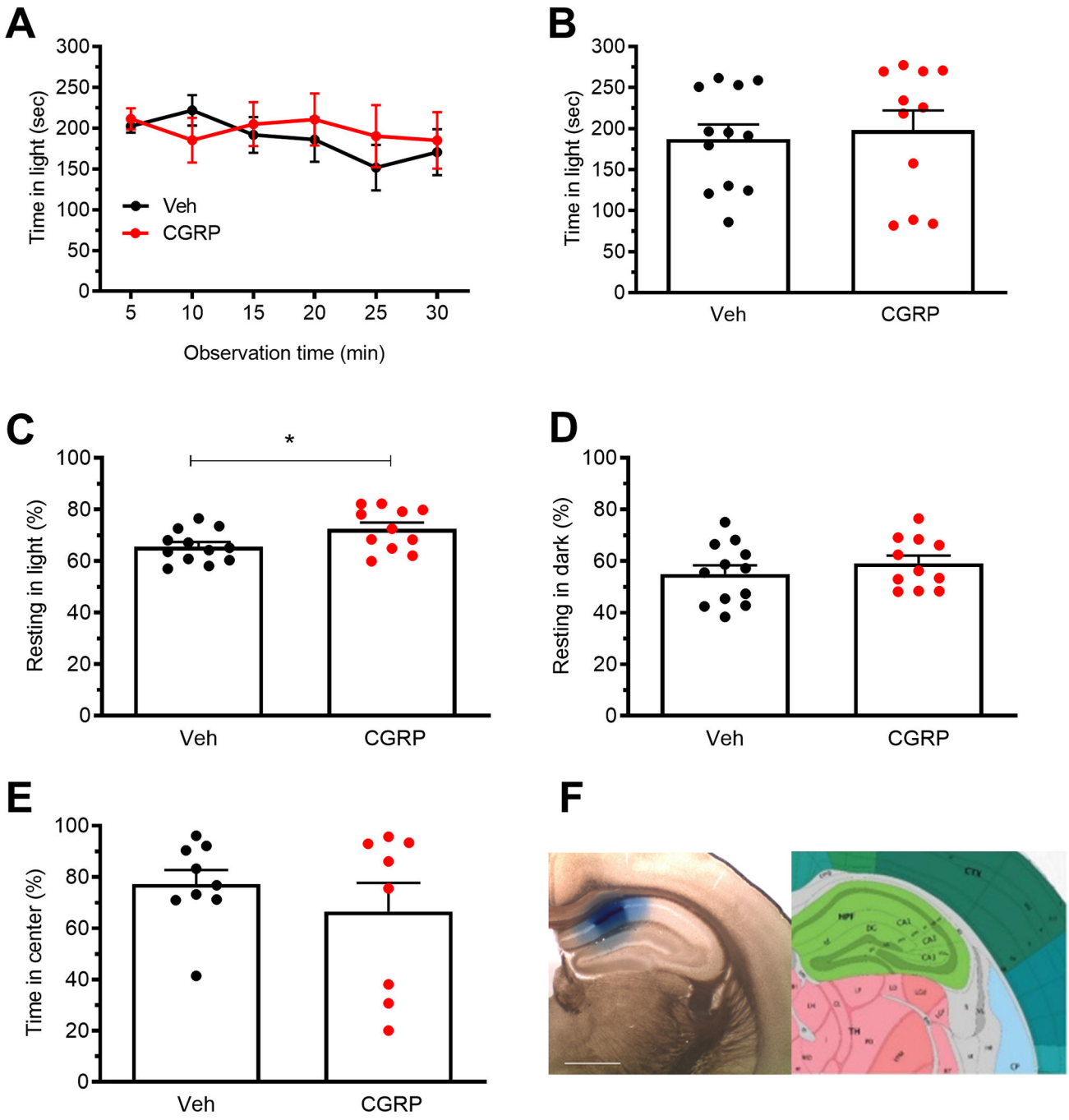

Figure 8. Injection of CGRP into the dorsal hippocampus does not induce light-aversive behavior.

A. Time in light over a 30 min light/dark box trial following injection of CGRP into the dorsal hippocampus. All mice in panel A are analyzed in panels B, C, D. **B.** Mean time in light per 5 min block of individual mice from A. C. Time resting in light during the assay. **D.** Time resting in dark during the assay. E. Time in center during the open field assay. **F.** Left: site of injection of Evans blue dye. Right: Allen Mouse Brain Atlas coronal image (image 74/132) representative of injected area. Image credit: Allen Institute. Scale bar = 1000 μm.

All error bars are SEM. *p < 0.05, see Table 1 for statistical analysis. A-D: Veh n=12, CGRP n=11. E: eYFP n=10, ChR2 n=11

Table 1:

Statistical Analysis

Fig. #	Analysis type and animal numbers
1A-D	At 55 lux: eYFP n=8, ChR2 n=11; At 2.7 × 10^4 lux: eYFP n=12, ChR2 n=18
1A	A three-way ANOVA revealed no statistical difference between light intensity: F (1,45) = 0.524, p = 0.47. Therefore, a two-way ANOVA was done to analyze treatment and time. Two-way ANOVA: At 55 lux: Interaction: F(5,85)=0.6434, p=0.67; Treatment: F(1,17)=14.41, p=0.001; Time: F(5,85)=0.1571, p=0.98. Holm-Sidak's multiple comparisons test: *p<0.05, ** p<0.01. At 2.7 × 10^4 lux: Interaction: F(5,140)=0.318, p=0.90; Treatment: F(1,28)=11.67, p=0.002; Time: F(5,140)=0.842, p=0.52. Holm-Sidak's multiple comparisons test: #p<0.05
1B	Unpaired two-tailed t-test: At 55 lux: t=3.80, df=17, p=0.001; At 2.7 × 10^4 lux: t=3.42, df=28, p=0.002
1C	Unpaired two-tailed t-test: At 55 lux: t=0.24, df=17, p=0.81; At 2.7 × 10^4 lux: t=0.25, df=28, p=0.81
1D	Unpaired two-tailed t-test: At 55 lux: t=2.17, df=17, *p=0.044; At 2.7 × 10^4 lux: t=2.76, df=28, p=0.009
1E	Unpaired two-tailed t-test: t=0.97, df=15, p=0.35; eYFP n=8, ChR2 n=9
3A-D	Veh n=26, CGRP 1.0 μg n=9, 0.5 μg n=13, 0.1 μg n=13
3A	Two-way ANOVA: Interaction: F(15,285)=2.147, p=0.0083; Treatment: F(3,57)=4.842, p=0.0045; Time: F(5,285)=3.381, p=0.006. Holm-Sidak's multiple comparisons test: ***p<0.001, **p<0.01, *p<0.05 CGRP 1.0 μg vs Veh; $^{\#\#}$p < 0.01, $^{\#}$p<0.5 CGRP 0.5 μg vs Veh; ^p<0.05 CGRP 0.1 μg vs Veh
3B	One-way ANOVA: F(3,57)=6.045, p=0.001. Holm-Sidak's multiple comparisons test: ***p<0.001, #p<0.05, ^p<0.05
3C	One-way ANOVA: F(3,57)=3.311, p=0.026. Holm-Sidak's multiple comparisons test: #p<0.05
3D	One-way ANOVA: F(3,57)=3.451, p=0.022. Holm-Sidak's multiple comparisons test: **p<0.01
3E	Unpaired two-tailed t-test: t=1.13, df=18, p = 0.27,; Veh n=9, CGRP n=11
5A-D	eYFP n=9, ChR2 n=10
5A	Two-way ANOVA: Interaction: F(5,85)=3.06, p=0.014; Treatment: F(1,17)=5.608, p=0.030; Time: F(5,85)=10.06, p<0.001. Holm-Sidak's multiple comparisons test: *p<0.05
5B	Unpaired two-tailed t-test: t=2.13, df=17, p=0.047
5C	Unpaired two-tailed t-test: t=1.171, df=17, p=0.26
5D	Unpaired two-tailed t-test: t=4.004, df=17 p<0.001
5E	Unpaired two-tailed t-test: t=7.025, df=14, p<0.001; eYFP n=6, ChR2 n=10
6A-F	Veh n=14, CGRP n=22
6A	Two-way ANOVA: Interaction: F(5,55)=0.109, p=0..99; Treatment: F(1,11)=0.136, p=0.72; Time: F(5,55)=1.664, p=0.16.
6B	Unpaired two-tailed t-test: t=0.952, df=34, p=0.35
6C	Unpaired two-tailed t-test: t=0.983, df=34, p=0.33
6D	Unpaired two-tailed t-test: t=1.25, df=34, p=0.22
6E	Unpaired two-tailed t-test: t=0.23, df=16, p=0.83; Veh n=9, CGRP n=9
7A-D	eYFP n=11, ChR2 n=11
7A	Two-way ANOVA: Interaction: F(5,100)=3.03, p=0.014; Time: F(5,100)=0.471, p=0.80; Treatment: F(1,20)=0.127, p=0.73
7B	Unpaired two-tailed t-test: t=0.356, df=20, p=0.73
7C	Unpaired two-tailed t-test: t=0.293, df=20, p=0.77
7D	Unpaired two-tailed t-test: t=1.340, df=20, p=0.20
7E	Unpaired two-tailed t-test: t=1.10, df=19, p=0.29, eYFP n=10, ChR2 n=11
8A-D	Veh n=12, CGRP n=11
8A	Two-way ANOVA: Interaction: F(5,105)=1.039, p=0.40; Time: F(5,105)=1.384, p=0.24; Treatment: F(1,21)=0.128, p=0.72
8B	Unpaired two-tailed t-test: t=0.358, df=21, p=0.72

Fig. #	Analysis type and animal numbers
8C	Unpaired two-tailed t-test: t=2.288, df=21, p=0.033
8D	Unpaired two-tailed t-test: t=0.901, df=21, p=0.38
8E	Unpaired two-tailed t-test:, t=0.306, df=19, p=0.76, eYFP n=10, ChR2 n=11